JOURNAL OF GEOPHYSICAL RESEARCH, VOL. 85, NO. C6, PAGES 3264–3276, JUNE 20, 1980

# The Statistical Prediction of Beach Changes in Southern California

DAVID G. AUBREY

*Woods Hole Oceanographic Institution, Department of Geology and Geophysics, Woods Hole, Massachusetts 02543*

DOUGLAS L. INMAN AND CLINTON D. WINANT

*Scripps Institution of Oceanography, Shore Processes Laboratory, La Jolla, California 92093*

Changes in natural sand beaches induced by variations in incident waves were predicted by techniques of linear statistical estimation and empirical eigenfunction analysis. A 5-year set of measured beach profiles and wave statistics from southern California constituted the data base for this two-faceted statistical study. First, daily beach profile changes were predicted using four different spectral representations of the wave field. These profile changes were predictable using spectral representations of wave energy, radiation stress, energy flux, and wave steepness. Because of constraints on statistical reliability, a longer data set is required to select one of these as an optimal wave parameterization. Second, weekly beach profile changes were predicted using weekly averaged wave characteristics. Weekly beach changes were predictable using weekly mean and maximum values of wave energy and wave height. The best predictor of those tested was the weekly mean wave energy. When combined with a longshore transport model, this onshore/offshore transport estimator should be applicable to other coastal regions with different beach and wave characteristics.

## INTRODUCTION

Predictions of the magnitude and direction of nearshore sediment transport suffer from the complexity of nearshore dynamics. The theory of nearshore sediment transport is not refined to a degree that enables the magnitude and direction of all sediment motion to be predicted, given a knowledge of the driving function. In addition it is not possible to predict what the exact nearshore driving force will be given deepwater conditions because of the lack of understanding of the interaction and shoaling of nearshore waves and currents. Thus even if a proven nearshore sediment transport model existed, the knowledge of nearshore driving forces would be inadequate to apply that model to predict sediment transport if only deepwater wave conditions are known. Since the dynamics of the nearshore zone are not adequately understood, statistical or empirical methods can be gainfully applied to the prediction of nearshore sediment transport. This paper describes one predictive technique and its application to nearshore sand level changes.

In the past, net changes in nearshore sediment distribution have been monitored by beach profiling techniques. The beach profile (elevation as a function of distance offshore) is sampled at a given rate over a period of time. The beach profile technique is important because it represents the one available technique for measuring net nearshore changes. It will lose its utility only when the theoretical advances have been made which will enable one to extrapolate large-scale erosional and depositional patterns from point measurements of sediment transport. The net profile changes may result from any combination of onshore/offshore sediment transport and divergences in longshore sediment transport. Although this study assumes that the dominant beach changes result from onshore/offshore sand transport, the model can be generalized by combining it with a longshore transport model.

Sediment movement in the nearshore is characterized by a wide variety of time scales. On the finest scales, sediment motion is associated with the turbulent fluctuations within the wave boundary layer. Daily and weekly beach fluctuations are associated with longer-period fluctuations in the wave conditions due to tidal or climatological phenomena. Seasonal beach changes arise from seasonal patterns in the wave field related to changes in meteorological forcing of the waves. Beach fluctuations with periods of 1 year or more can be associated with long-term climatic conditions or interrruptions in the sediment supply, for example. In this study the statistical prediction of daily and weekly changes in the beach configuration is examined. The data sets were not long enough to consider yearly changes and were not adequately sampled to look at changes with scales finer than 1 day or 1 week. Linear statistical estimation was applied to both daily and weekly beach changes (as represented by empirical eigenfunction analysis) in hindcast and forecast modes. (A hindcast is a regression estimate which determines the optimal relationship between known beach changes and the driving force. A forecast is an estimate of future beach changes derived from a known driving force and a predetermined statistical relation between beach changes and driving forces.) Beach changes were predicted, using different parameterizations of the incident wave field.

## STATISTICAL TECHNIQUES

### *Linear Statistical Predictors*

The simplest predictor relates the data in a linear fashion to the quantity to be predicted (the predictand):

$$\mathbf{P} = \mathbf{A}\,\mathbf{D} \qquad (1)$$

where $\mathbf{P}$ is the $(m \times N)$ matrix of the $m$ quantities to be predicted, $\mathbf{D}$ is the $(n \times N)$ matrix of $n$ data parameters, and $\mathbf{A}$ is an $(m \times n)$ coefficient matrix. $N$ is the total number of observations used in the prediction. Although this predictor is linear, the data themselves, $\mathbf{D}$, can be complicated nonlinear functions of the measured quantities, which are then related linearly to the predictand.

To form a minimum error variance estimator, the diagonal elements of the error covariance matrix $\mathbf{C}_e$ are minimized:



Paper number 9C1749.
0148-0227/80/009C-1749$01.00

$$\mathbf{C}_e = \langle(\hat{\mathbf{P}} - \mathbf{P})(\hat{\mathbf{P}} - \mathbf{P})^T\rangle \quad (2)$$

where $T$ denotes the matrix transpose, and the angle brackets denote an ensemble average. Given this criterion the Gauss-Markov theorem defines the form of the optimal estimate:

$$\hat{\mathbf{P}} = \mathbf{C}_{PD}\mathbf{C}_{DD}^{-1}\,\mathbf{D} \quad (3)$$

where $\mathbf{C}_{PD}$ is the covariance matrix between the predictand and the data and $\mathbf{C}_{DD}$ is the autocovariance matrix of the data. No other linear estimator of the form (1) yields a smaller mean square error [*Liebelt,* 1967; *Davis,* 1976, 1977].

This linear estimator is used in both a hindcast and a forecast sense. For our purposes a hindcast is a prediction that generates its own optimal coefficient matrix **A**. A forecast is a prediction based on an independent prediction matrix **A**.

A measure of prediction utility is the hindcast skill, which is related to the ratio of the error covariance diagonal elements and the diagonal terms of the predictand covariance matrix. The hindcast skill for one element $P_i$ of the predictand is

$$S_H = 1 - \frac{(\hat{P}_i - P_i)\quad(\hat{P}_i - P_i)^T}{\langle P_i P_i^T\rangle} \quad (4)$$

By combining (2) and (4), $S_H$ is shown to be dependent upon the square of the sample mean products, so any chance connection between the predictand and the data will increase the hindcast skill. Finite record lengths and sampling errors also affect the artificial predictability of the estimator. *Davis* [1976, 1977] shows the artificial predictability to be a function of the ratio of the number of data parameters, $n$, and the number of observations, $N$. This artificial skill, proportional to $n/N$, reduces the forecast skill by approximately the same amount as the hindcast skill is increased due to artificial predictability [*Davis,* 1977].

A useful measure of prediction skill is the mean-square-forecast error (MSFE), obtained by summing the errors of each forecast element $P_{ij}$:

$$(\text{MSFE})_i = \sum_{j=1}^{N} (\hat{P}_{ij} - P_{ij})^2 \quad (5)$$

This is the MSFE for the $i$th row of the predictand. To obtain an estimate of the 'goodness' of fit, (5) is normalized by the mean square value (MSV) of the $i$th predictand quantity:

$$(\text{MSV})_i = \sum_{j=1}^{N} (P_{ij})^2 \quad (6)$$

The new 'normalized' error estimate is the basis for judging the predictor. If the normalized error is greater than one, then the predictor performs more poorly than an estimate based solely on the mean. If the normalized error is less than one, the new predictor out performs that predictor based on the mean. Suitable tests must be made to calculate confidence limits for the prediction.

One way to reduce the degradation in forecasting ability is to reduce artificial predictability by ensemble averaging over all available realizations of the process (providing the data sets have the same size, sampling interval, etc.). Unfortunately, in geophysics, observations are generally so scarce this is rarely possible. Another method is to increase the number of observations, $N$, of each sample to approximate better the true covariances by the sample mean products. A third method is to reduce the number of data parameters to a few more relevant measures and thereby reduce the artificial hindcast skill. In this study, objective ranking with empirical eigenfunction analysis was used to reduce the number of data variables.

### *Empirical Eigenfunctions*

*Lorenz* [1959], *Davis* [1976], and others have applied empirical eigenfunction analysis to some geophysical problems. *Resio et al.* [1974] and *Winant et al.* [1975] have successfully applied this technique to beach data (see also numerous subsequent articles by the same authors). *Vincent and Resio* [1977] applied the technique to time series of wind wave spectra. The empirical eigenfunction solution represents an expansion of the data with two sets of orthonormal functions:

$$h(x, t) = \sum_{l=1}^{N} c_l(t)e_l(x)(\lambda_l n_x n_t)^{1/2} \quad (7)$$

where $c_l(t)$ are functions of time only, $e_l(x)$ are functions of space only, $\lambda_l$ are the eigenvalues of the data sum of squares and cross products matrix, and $n_x$ and $n_t$ represent the number of points in space and time, respectively. The elements $h(x, t)$ could represent time series of beach profiles or wave spectra, for instance. By forcing the functions to be orthonormal, and requiring the functions to be ordered to explain best the variability of the data in a least squares sense, all $\lambda_l$, $c_l(t)$, and $e_l(x)$ can be easily determined [e.g., *Aubrey,* 1978, 1979].

These functions have the following useful properties:

1. Empirical eigenfunctions provide the most efficient method of compressing the data. That is, they provide the most dense representation of a data set in the sense that the first $n$ terms in the expansion explain more of the data variability than the first $n$ terms of any other expansion.

2. Since both the spatial and the temporal eigenfunctions are orthogonal sets, each corresponding set ($\lambda_l$, $e_l$, $c_l$) may be regarded as representing a mode of variability which is uncorrelated with any other mode.

3. The eigenfunction representation is conveniently applied to minimum mean square error estimation by providing a useful a priori method for reducing the number of variables and also providing a way to remove the noise (or less predictable part of the data) from the data set.

*Aubrey* [1978, 1979] presented examples of the application of this analysis to beach profile data, where a (100 × 44) data matrix was efficiently represented by a (5 × 44) matrix of eigenfunctions. *Vincent and Resio* [1977] show a similar reduction in data size and complexity for wave spectra. Although difficult to interpret physically in some cases, the eigenfunction representation is a valuable tool in estimation theory.

## THE DATA

The data analyzed consist of measurements of beach profiles and surface gravity waves at Torrey Pines Beach, California. This site was selected both for its accessibility and because it is a long, relatively straight stretch of sandy beach with uncomplicated offshore bathymetry (it is located far enough north that the Scripps-La Jolla submarine canyon system does not significantly affect the local gravity wave field).

Three primary range lines (North range (NR), Indian Canyon range (IC), and South range (SR)) were established in June 1972 and were measured on at least a monthly basis until 1978 (Figure 1) [*Nordstrom and Inman,* 1975; *Aubrey et al.,* 1976]. Four additional range lines (ranges A, B, C, and D) were established in February 1977 and were monitored only

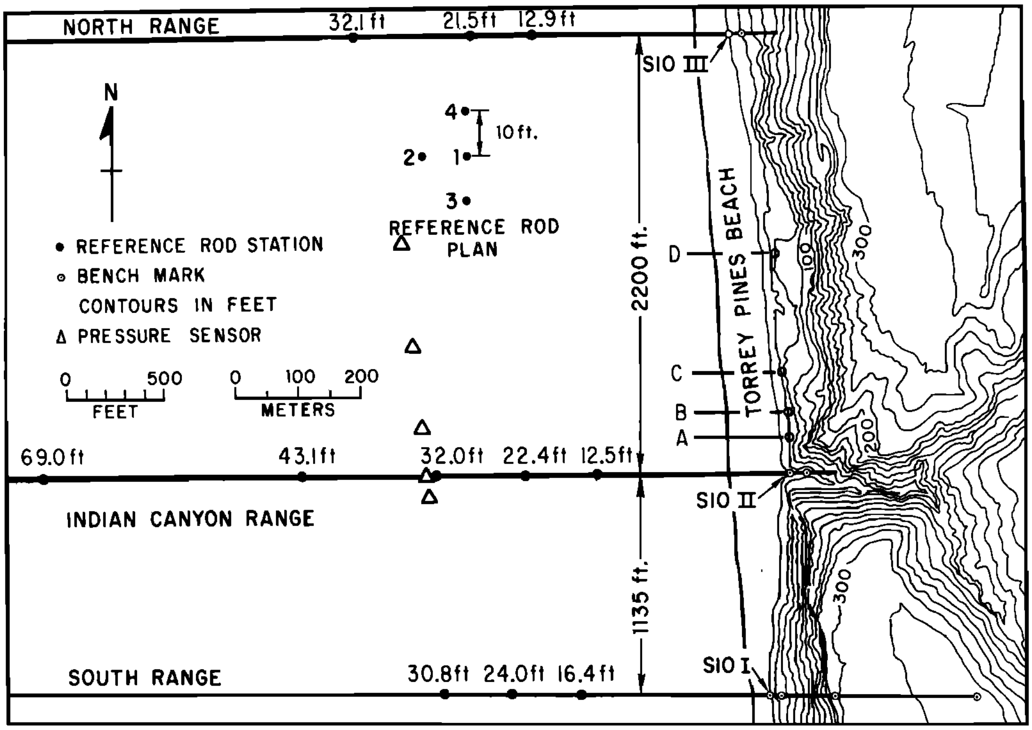


Fig. 1. Map of range line locations and reference rod locations at Torrey Pines Beach.

during that spring. The range lines are referenced to a U.S. Coast and Geodetic Survey benchmark [*Aubrey*, 1978, 1979].

Beach profiles were measured by using techniques described by *Inman and Rusnak* [1956] and *Aubrey* [1978]. Onshore surveys to mean approximately lower low water were done at low tide, using a surveyor's level and rod to determine elevation at 10-foot horizontal intervals. The offshore surveys combined several techniques. An offshore profile was first made with a fathometer out to depths of 20 m on the same day as the onshore survey, but at high tide. Since the errors in a fathometer survey are often 30 cm or more [e.g., *Inman and Rusnak,* 1956], an accurate method for correcting the offshore fathometer survey was used. Arrays of brass reference rods approximately 1.25 m long, installed at known locations along each profile (Figure 1), were measured each month by divers, yielding a relative change in sand level from month to month. With these measurements, which have a potential accuracy of 1 or 2 cm, the fathometer records were corrected [*Aubrey,* 1978, 1979].

Measurements of surface gravity waves were made along Indian Canyon range at a depth of approximately 9.3 m (Figure 1), using a linear array of pressure sensors with a telemetering link to the Shore Processes Laboratory at Scripps Institution of Oceanography [*Lowe et al.*, 1972]. Since extensive linear wave refraction tests indicated that the offshore bathymetry produces no major differences in wave refraction along this limited coastline, the same wave data was used for all range lines. In this study, only frequency spectral estimates were used, although directional estimates could be derived from these data [*Pawka et al.*, 1976]. The spectral estimates had 32 degrees of freedom, with a record length of 2048 s, a sample rate of 0.5 s, and a frequency resolution of 0.0078125 cps. Frequencies above 0.25 Hz were suppressed in the analysis because of the depth attenuation of waves in 9.3 m of water; this helped reduce spectral aliasing. The reliability of the estimates was increased by averaging the estimates from each of the sensors, in an ensemble sense, assuming homogeneity of the wave field.

When the array data were not available, daily visual estimates of the significant wave period and wave height, or spectral estimates made from a single pressure sensor at the end of the SIO pier [*Seymour and Sessions*, 1976] were used instead [*Aubrey*, 1978]. Although neither of these latter sources is as desirable as the linear array data, they do provide rough estimates of wave energy.

The prediction study examined two major time scales of beach change. The first data set was a month-long series of beach profiles sampled at daily intervals, while the second was a $1\frac{1}{2}$-year series of profiles, sampled at approximately weekly intervals. The wave statistics were well known for the month-long sample; for the longer sample only certain averages of the wave statistics were used as input. This two-faceted scheme was designed to determine (1) what the best spectral estimators of beach changes are, and (2) what averaged wave statistics yield the best predictions.

The predictands always consisted of a representation of the beach profile time series (Figure 2), while the data parameters consisted of various wave parameterizations. To characterize beach profile changes efficiently and concisely, the profiles were represented by their empirical eigenfunctions, which retain spatial covariance information. The predictand is formed from the temporal dependence $c_i(t)$ of the first few dominant eigenfunctions, here called beach eigenfunctions (BEF).

The mean beach profile was removed from the profile data before calculating the eigenfunctions to improve the prediction results in three ways: (1) The data matrix need not contain a constant to predict the mean profile time variation. (2) Less artificial variation is introduced into the higher eigenfunction modes. (3) Predictor skill is increased since a small

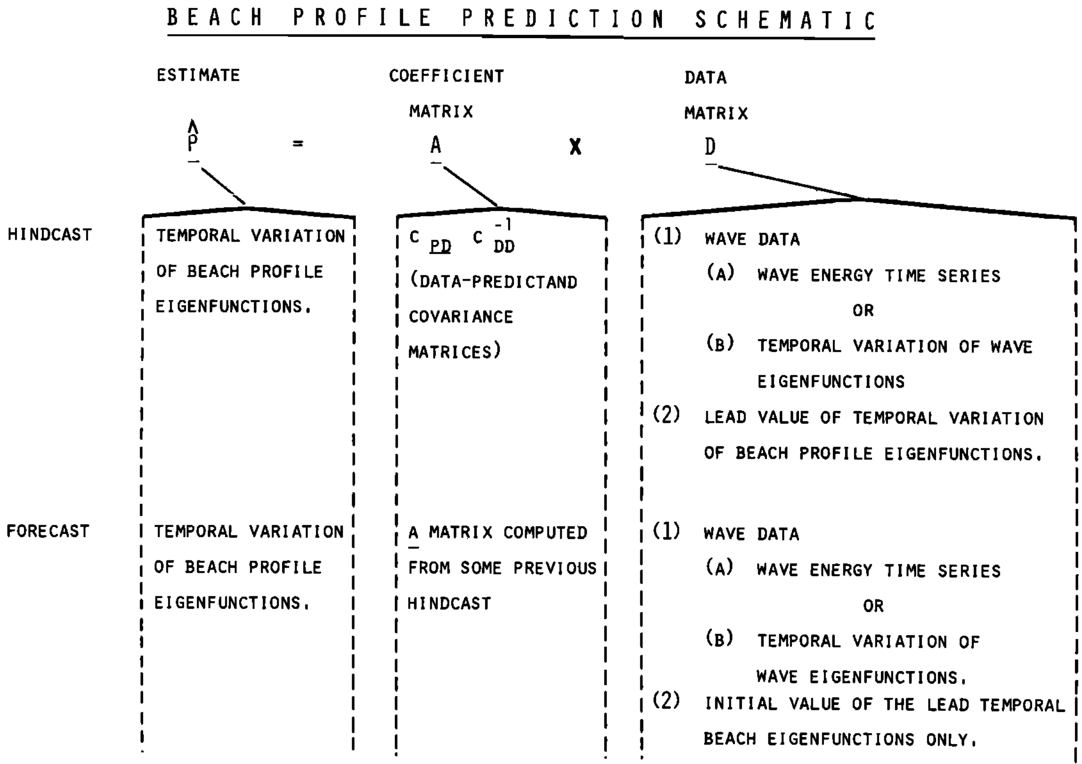


Fig. 2. Description of the elements and methodology used in the minimum error variance estimate of beach profile changes.

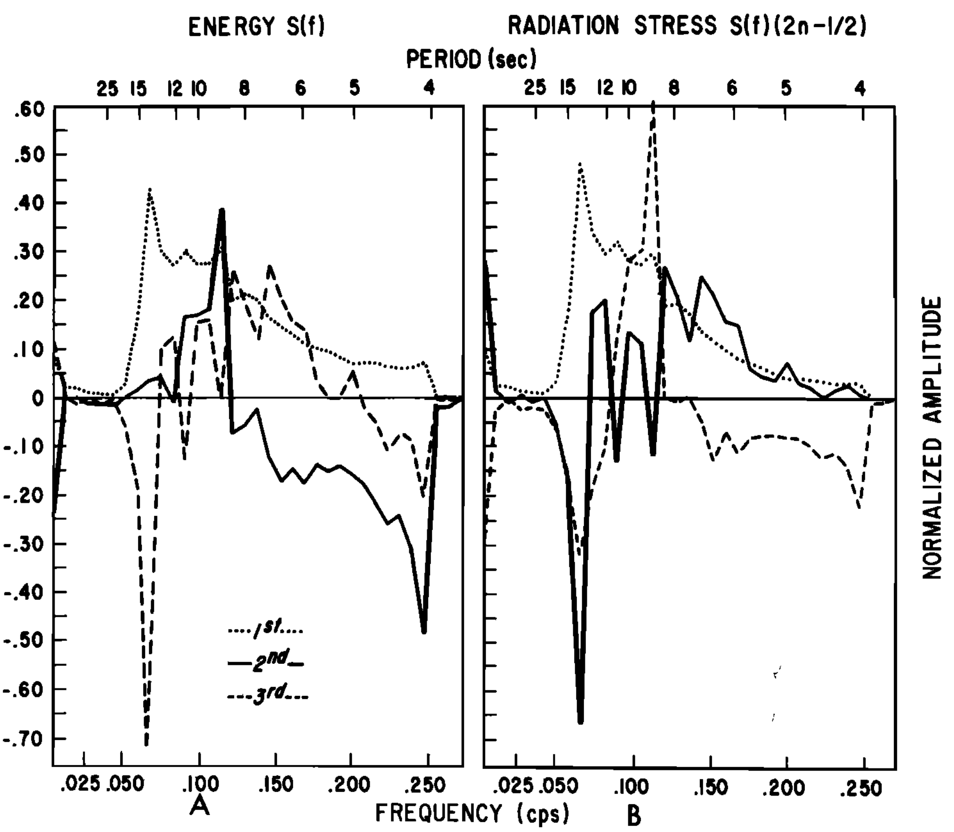


Fig. 3. Wave eigenfunctions for (*a*) wave energy and (*b*) radiation stress, as a function of wave frequency.

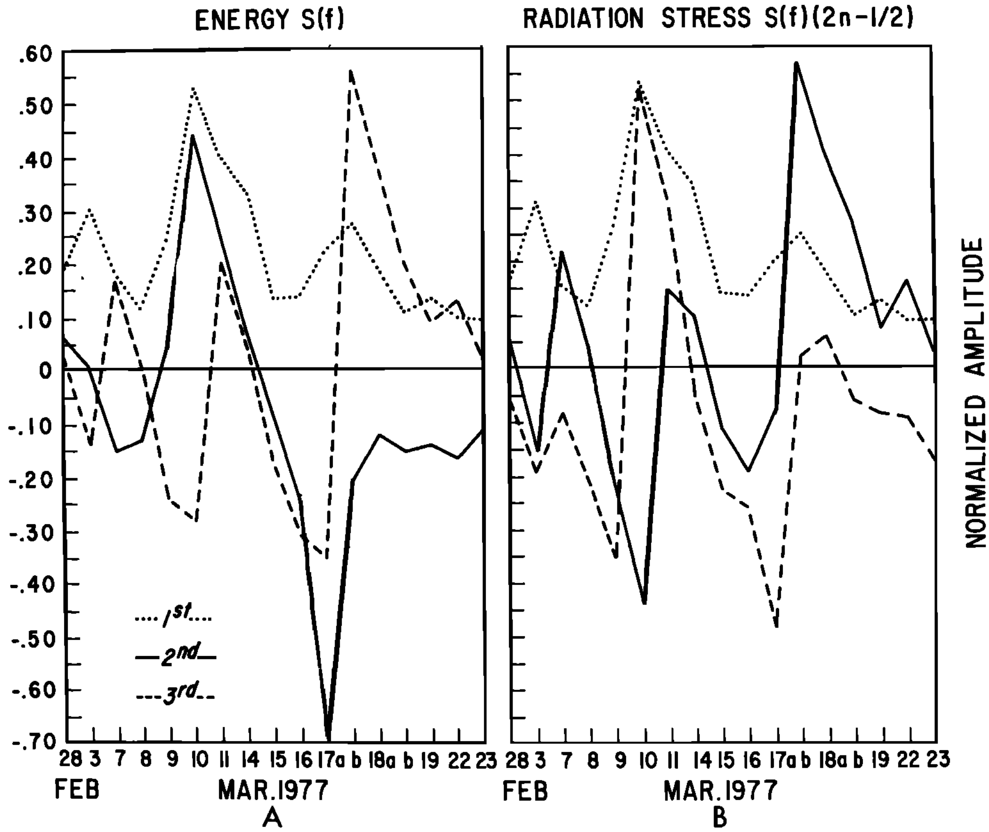


Fig. 4. Temporal structure of the wave eigenfunctions for (*a*) wave energy and (*b*) radiation stress, for the March 1977 wave data.

error in forecasting the time dependence of the first eigenfunction represents a large error in the variance [*Aubrey*, 1978]. The mean beach profile was obtained from the entire 5-year sample of profile data [*Aubrey*, 1978, 1979] which showed no net accretion or erosion over the period of the study.

*Aubrey et al.* [1976] showed that distinct beach forms correlate well with different types of waves. When storm waves act on a berm profile, erosion occurs on the foreshore; yet, if the same waves act on a bar profile, little modification of the profile results. This factor complicates the prediction problem, since the covariation between the waves and the previous profile configuration becomes an important parameter. Therefore, any attempt to predict beach profile changes must involve a knowledge of not just the waves but also of the prior history of the beach. In this study the important prior history of the beach was assumed to be the preceding profile configuration. That is, the profile of the previous week (or the appropriate previous time period) was combined with the recent wave information to predict the new beach profile. This does not pose a problem in hindcasting, where the time history of the beach is already known and one is testing the maximum expected predictability of the process. The previous profile (which has been measured) is used as input data for computing the next profile. If the predictands are the eigenfunctions of the beach profiles, then the lead values of those same eigenfunctions are used. A problem arises when forecasting, however, since the time history of the profile variation is assumed to be unknown. The only profile which can be specified is the initial profile configuration. To apply the lead BEF concept, the computed profile configuration at each time step must be used as a data value for the next estimate. This can cause serious error propagation since errors in the profile estimate will be used as input data for the next estimate, thereby transmitting and amplifying the error continuously. If the forecast skill is low in the first place, this will deteriorate it even further.

## RESULTS AND DISCUSSION

### *Prediction of Daily Beach Profile Changes*

The first part of this study examined a series of beach profiles measured during an intensive field program in March 1977. Measurements of the incident wave field were collected generally 8 hours a day, from 0900 to 1700 hours, varying slightly according to the demands of the field experiments. Beach profiles were measured along seven range lines (Figure 1), generally extending to −1 m (MLLW) depth. Wave frequency spectral estimates were calculated for 34-min lengths of record and were transformed into either estimates of momentum flux, energy flux, or wave steepness. These estimates were averaged over periods corresponding to the time interval between beach profiles. These averaged estimates were formed into an array of time series of spectral estimates, consisting of 35 frequency bands and 17 time periods, with a frequency resolution of about 0.0078 cps.

To represent concisely and efficiently their variability, the empirical eigenfunctions of the wave data were calculated from a sum of squares and cross products matrix $\mathbf{C}_f$ [e.g., *Vincent and Resio*, 1977]:

$$\mathbf{C}_f = \mathbf{S}(f, t) \cdot \mathbf{S}(f, t)^T \qquad (8)$$

where $\mathbf{S}(f, t)$ is the array of spectral time series of different fre-

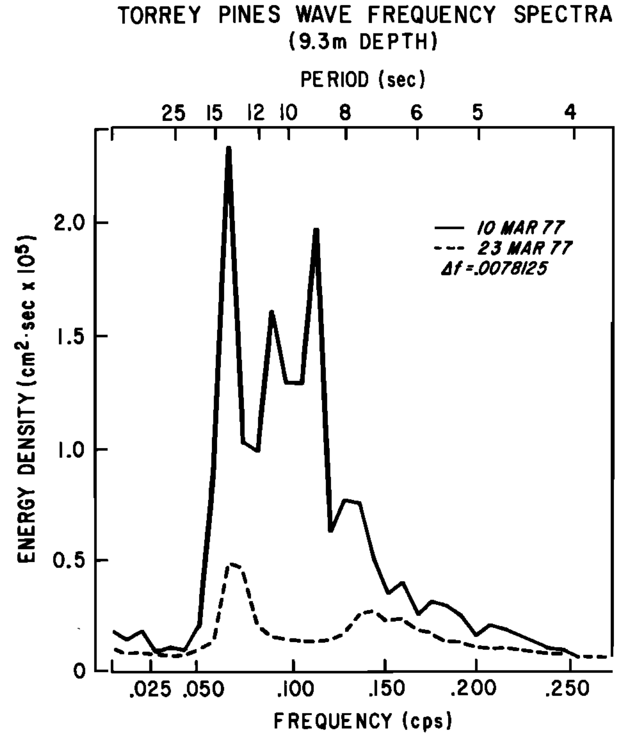


Fig. 5. Two examples of wave frequency spectra from March 1977. The two spectra represent a high-energy wave field and a low-energy wave field.

quency bands and the superscript $T$ refers to the transpose operator. The eigenvalues and eigenfunctions of the above matrix were then calculated to examine the empirical structure of the wave field. The temporal dependence of these functions, $c_i(t)$, were used as data parameters in the linear prediction of beach profile changes and are called wave eigenfunctions (WEF).

The four wave parameterizations examined were the onshore component of the radiation stress [*Longuet-Higgins and Stewart,* 1964; *Bowen et al.,* 1968], the energy flux, the wave steepness, and the energy spectrum. Each has been used in the past with varying degrees of success to describe some aspect of nearshore forcing and were obtainable from the available wave data. In this study the radiation stress was approximated as the onshore flux of onshore directed momentum, for the case of normal wave incidence

$$S_{xx}(f, t) \sim S(f, t) \cdot (2n - 1) \tag{9}$$

Here $S(f, t)$ is the portion of the variance associated with frequency $f$, and $n$ is the ratio of group to phase velocity. The energy flux was represented by

$$ECn(f, t) \sim S(f, t) \cdot C \cdot n \tag{10}$$

where $C$ is the phase velocity. The wave steepness was represented by

$$H/L(f, t) \sim [S(f, t)]^{1/2}/L(f, t) \tag{11}$$

where $L$ is the wavelength. The wave energy is represented by $S(f, t)$. The true value of the parameter can be found from the representation in all four cases simply by multiplying by a constant. Since the absolute magnitude is not important in the prediction process (all data parameters are normalized), the deletion of the constant has no effect on the prediciton.

The wave field underwent significant changes over the period of the study (Figures 3–5), as is reflected in the wave eigenfunctions for the different wave parameterizations. For all four wave parameterizations, the first WEF dominates the

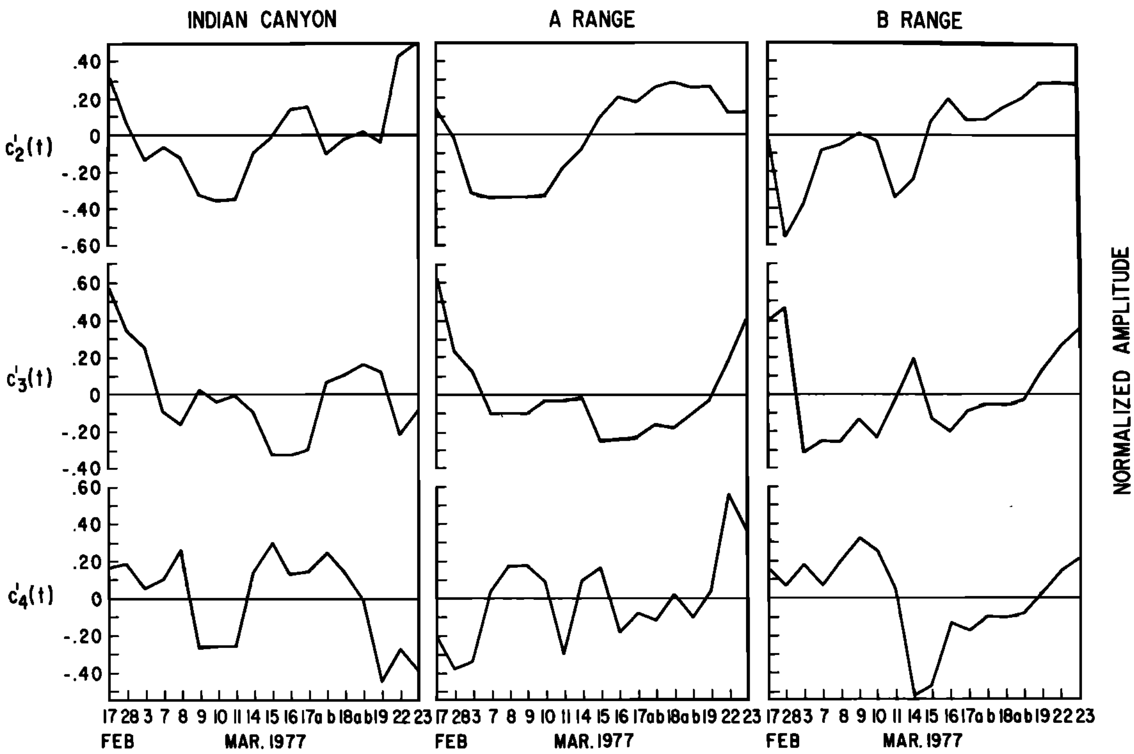


Fig. 6. The temporal structure of the empirical eigenfunctions for Indian Canyon, A, and B ranges for the period of March 1977. The mean profiles have been removed from the data sets.

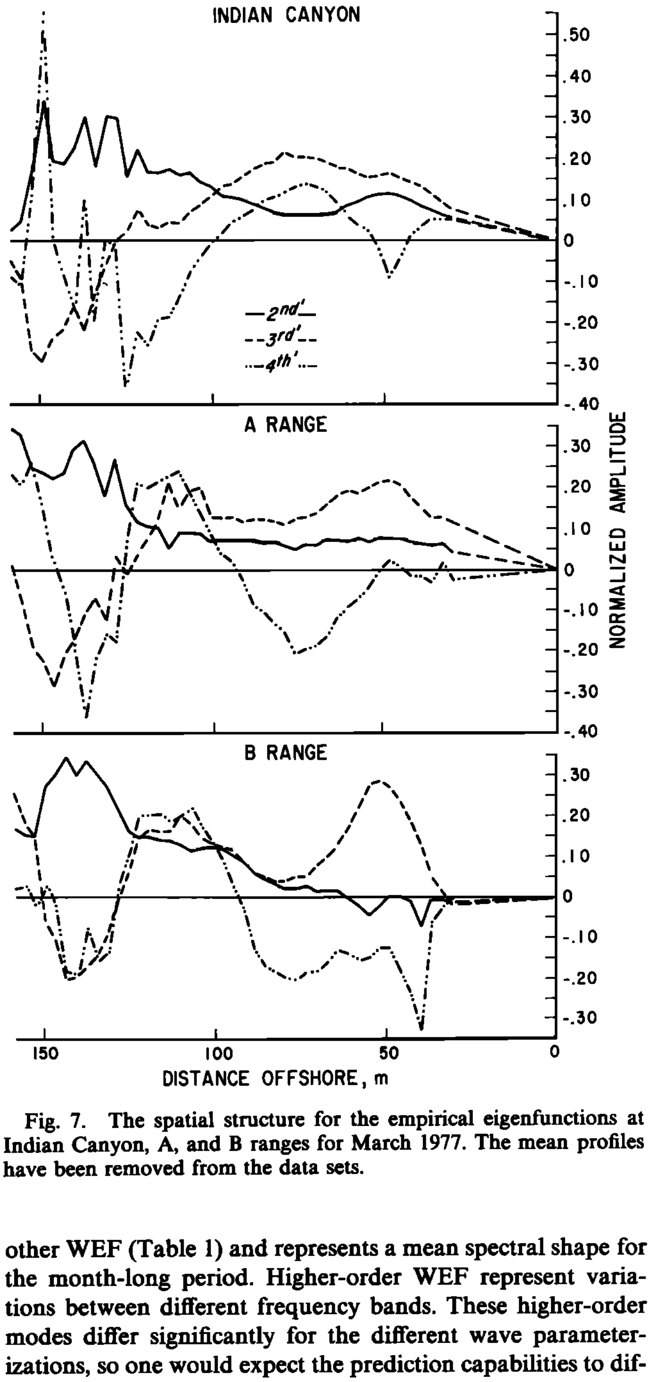


Fig. 7. The spatial structure for the empirical eigenfunctions at Indian Canyon, A, and B ranges for March 1977. The mean profiles have been removed from the data sets.

other WEF (Table 1) and represents a mean spectral shape for the month-long period. Higher-order WEF represent variations between different frequency bands. These higher-order modes differ significantly for the different wave parameterizations, so one would expect the prediction capabilities to differ between them. The radiation stress and energy flux estimates tend to enhance low frequencies and suppress high frequencies. The wave steepness estimate emphasizes the high frequencies [*Aubrey*, 1978].

The raw frequency spectra varied markedly during the experiment as well (Figure 5). The high and low wave conditions during this period can be compared to the WEF as a more physical feeling of the wave eigenfunctions (Figures 3 and 5).

Since only 18 profiles at each location were measured during the March field experiment, statistical reliability is low. To increase reliability, two profile sequences were formed from the beach eigenfunctions. Temporal eigenfunctions for ranges IC, A, and B were merged end-to-end to form a time series of profiles, representing three realizations of profiles responding to the same forcing function. The second profile sequence consisted of C, D, and North ranges. The temporal BEF for each of these ranges were calculated separately and then placed into their proper sequence (Figure 6). Figure 7 shows the spatial structure of the BEF for one of the groups. In these figures the mean profile was removed to characterize only deviations from the mean. Removal of the sample mean introduces some errors since the population mean is not well known for ranges A, B, C, and D. Because of the preliminary nature of this study, this error will not seriously affect the major results; however, it does limit comparison with similar predictions elsewhere. Since the mean profile was removed from the data set prior to this eigenfunction analysis, the lowest-order eigenfunction is analogous to the seasonal function, or BEF 2. This lowest-order eigenfunction is labeled 2nd' (solid curve) to preserve the similarity between eigenfunctions of the sum of squares and cross products matrix and the covariance matrix.

The first few BEF for all six profiles exhibit similar spatial structures (e.g., Figure 7). The first BEF (2nd') dominates the other eigenfunctions, in terms of explained variance (Table 2), so efforts are concentrated on predicting this quantity. The spatial structure of the higher-order eigenfunctions are not consistent for all six ranges, so one should not expect any significant skill in predicting these functions.

To obtain estimates of the predictand, hindcasts were made by using the WEF and the lead BEF as data values. For various combinations of the number of WEF and lead BEF, the coefficient matrix A was obtained. Then a forecast was made on that profile grouping not used to estimate A. For example, hindcasts were first made on the profile grouping consisting of ranges IC, A, and B, and matrix A was calculated. This matrix was then used to forecast the profile changes for the profile grouping consisting of *C*, *D*, and North ranges. The forecast in this case involved different profiles; however, the same wave data used to form the hindcast was used in the forecast. In this

TABLE 1. Percent of the Mean Square Value of the Data Explained by the Characteristic Wave Functions for Four Wave Parameterizations

| | Energy | Radiation Stress | Energy Flux | Steepness |
|---|---|---|---|---|
| WEF | | | | |
| 1 | 87.7 | 89.6 | 89.8 | 94.8 |
| 2 | 4.6 (37.6) | 3.5 (33.4) | 3.5 (33.9) | 3.9 (76.0) |
| 3 | 3.2 (26.2) | 2.8 (27.2) | 2.8 (27.1) | 0.5 (9.7) |
| 4 | 2.0 (16.0) | 1.7 (16.5) | 1.7 (16.4) | 0.21 (4.0) |
| 5 | 1.0 (8.1) | 0.9 (9.0) | 0.9 (9.1) | 0.2 (3.6) |
| Total | 98.5 | 98.6 | 98.6 | 99.7 |

Numbers in parentheses are percents of residual mean square value explained after removing the first WEF; $n_x = 35$, $n_t = 17$.

TABLE 2. Percent of Variance Explained by the Second Through the Sixth Beach Eigenfunctions

| | Indian Canyon | A | B | C | D | North Range |
|---|---|---|---|---|---|---|
| BEF | | | | | | |
| 2′ | 67.5 | 73.2 | 52.8 | 72.7 | 67.8 | 74.9 |
| 3′ | 12.1 | 13.2 | 18.3 | 15.2 | 21.1 | 14.3 |
| 4′ | 7.1 | 5.5 | 14.0 | 4.2 | 4.7 | 5.0 |
| 5′ | 3.8 | 3.2 | 5.1 | 2.5 | 2.3 | 2.7 |
| 6′ | 3.5 | 2.1 | 4.7 | 2.1 | 1.6 | 1.0 |
| Total | 94.0 | 97.2 | 94.9 | 96.7 | 97.5 | 97.9 |
| Variance without 1st BEF, m$^2$ | 0.0179 | 0.0230 | 0.0195 | 0.0457 | 0.0101 | 0.0425 |
| Percent of total mean square value of data accounted for by 1st BEF | 98.21% | 97.95% | 98.90% | 96.19% | 99.36% | 98.53% |

The mean beach profile has been removed from the data, $n_x = 44$, $n_t = 18$.

sense the forecast is not a totally independent test of the forecast ability. It is useful, however, in an intercomparison of the different wave parameterizations and to demonstrate the absence of serious error propagation through time.

The results of this analysis demonstrate a trade off between the amount of information necessary for the forecast and the increase in artificial predictability. Once the number of data functions increases markedly, artificial predictability becomes important and reduces the forecast skill. The best predictor in each case is one which retains information only about the primary beach variability (the second BEF) but which also retains information on the fine structure of the wave field. For instance, by using the energy flux the best estimate of the mean beach function has five WEF and only one BEF.

Comparisons of the estimation results with predictand measurements show prediction trends (Figures 8 and 9). Extremes were poorly predicted, but mean trends were predicted well. Figure 8 is a hindcast estimate, with a low mean square error of 0.006 m$^2$. Figure 9 is a forecast estimate, with a higher mean square error of 0.010 m$^2$. The total mean square value of the predictand in both figures in 0.024 m$^2$. Table 3 lists the coefficient matrix A for the two cases, showing the weightings of each normalized WEF and lead BEF. The most important WEF is the second one, representing a high-frequency, low-frequency trade off (Figure 3*b*).

Table 3 can be used to evaluate the effect of wave steepness on beach profile changes. The second WEF, which is the most heavily weighted in both examples, is positively weighted in predicting the second BEF. A positive weighting of the second WEF for wave steepness corresponds to an increase in high-frequency wave steepness and a decrease in low frequency. This fact (combined with the weighting) suggests that low-frequency waves erode the beach and high-frequency waves accrete the beach, contrary to many laboratory results. The contradiction might be resolved when a longer data set becomes available for scrutiny or may indicate the seriousness of scaling problems in laboratory tests.

The primary result of this section is that daily beach profiles are predictable from a knowledge of the incident waves alone. The actual trends in prediction, such as the one mentioned in the previous paragraph, must be viewed as tentative since the data set is limited. A longer data set, spanning at least 1 year, is required before a useful coefficient matrix A is generated.

For the forecast only the initial value of the lead BEF is used as data. The new value of the predictand computed from this and the wave data is then used as a data value to calculate the next estimate. As was discussed previously, this provides an excellent means for error propagation. In fact, the estimates show no such trend in error growth, indicating that the

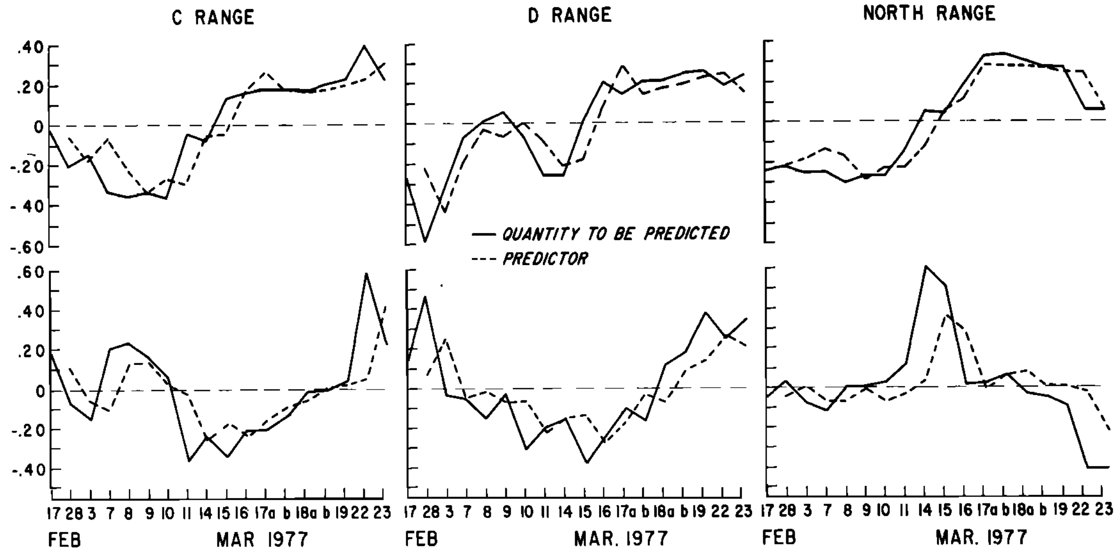


Fig. 8. A hindcast of the temporal beach eigenfunctions (BEF) at C, D, and North ranges for the March 1977 beach profiles. The input data consisted of the first two lead BEF and the first four WEF for the wave steepness estimates. The mean profiles have been removed from the beach data.

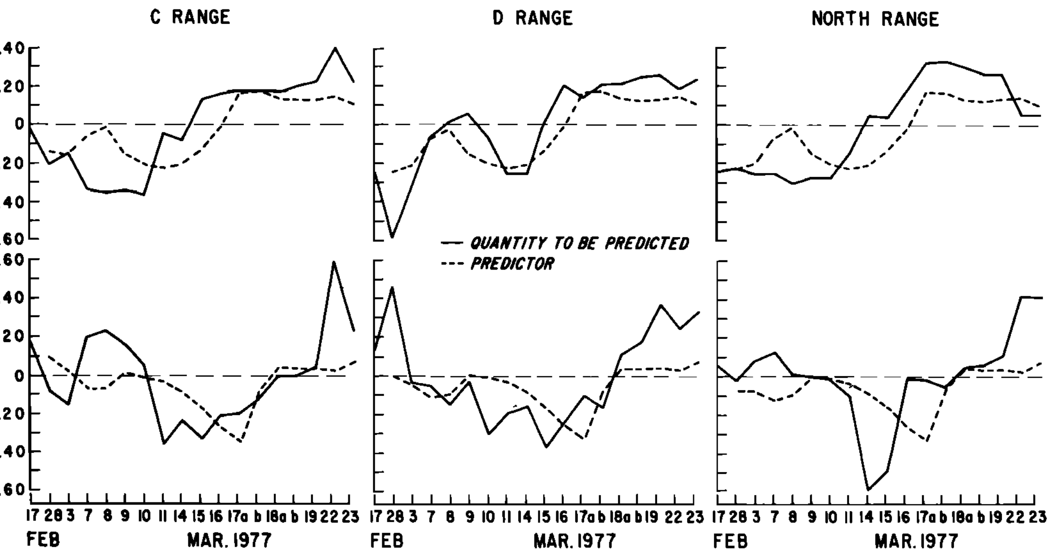


Fig. 9. A forecast of the temporal BEF for C, D, and North ranges for the March 1977 beach profiles. The input data consisted of the first two lead BEF and the first four WEF for the wave steepness estimates. The mean profiles have been removed from the beach data.

processes may not be unpredictable so much as coarsely predictable because of the limited data sample.

### *Prediction of Weekly Beach Profile Changes*

The previous section considered the prediction of daily beach profile changes by using a spectral representation of the incident waves. It is rare that either daily profiles or daily spectral wave information are available over any great length of time, so the predictability of weekly profile changes by using some averaged wave parameters was evaluated.

From the 5-year data set of profiles at Torrey Pines, a period of 1½ years (over which weekly beach surveys and daily wave estimates exist) was selected for study, using profiles from North range and South range. The profile sample was divided into two sections. The first was a 1-year-long section from December 1975 through January 1977; the second was a 6-month section from March 1975 through September 1975. The optimal predictor was calculated for both North range and South range for the 1-year-long sample and then used to forecast the changes for the 6-month-long data sample, as a measure of forecasting ability on an independent sample. In addition, the predictability could be examined between ranges to get an idea of the coherence of beach changes longshore. Then to increase the statistical reliability of the estimate, the 1-year and ½-year samples from North range were merged and were used to forecast changes at South range.

Four different input wave parameters were used to examine the weekly beach predictability: weekly estimates of the maximum weekly variance $E_m$; the square root of this quantity; the weekly mean energy variance $E$; and the square root of this quantity, that is, the root-mean-square wave height. The maximum value of the variance $E_m$ was chosen since observations have shown that a single storm can change the profile drastically, and any averaging would smear this single event [*Aubrey et. al.*, 1976]. The square root of the maximum weekly variance was used to test the hypothesis that it is not the energy but the wave height which is the dominant forcing quantity in the nearshore. The third quantity was the mean weekly energy variance $E$, consisting of equally weighted averages of all the wave records measured in the interval between two beach surveys. This quantity was selected to test whether average conditions, not extreme events, determine beach response. One might expect that the combination of the mean value and the extreme value of the variances would be a good predictor. The square root of the mean weekly variance (or the root-mean-square wave height) was chosen to test the idea again that it is the first power of the wave height, not the second, which is responsible for beach variability. *Aubrey* [1978, Appendix 2] lists the values of these different parameters used as data for the predictor.

The spatial structure of the BEF for North range for each of the two time periods is similar (Figure 10). The mean profiles were removed before the eigenfunctions were calculated for reasons previously mentioned. The dominant eigenfunction is still the seasonal beach function (Table 4).

The prediction proceeded by calculating the coefficient matrix **A** for one particular profile data set, using various combinations of wave parameters, and applying this result to forecast the changes for the other profile data sets. The forecast skills in all cases are significant (i.e., MSFE < MSV), indicating that beach profiles can be predicted from weekly estimates of the wave statistics, even over the period of 1 year. If the forecast were made only over shorter lengths of time, and the forecast were occasionally updated, then a better predictor would result. It is significant that in this forecasting method the errors did not propagate through the prediction; that is,

TABLE 3. Coefficient Matrices for Figures 8 and 9

| | Figure 8 | | Figure 9 | |
|---|---|---|---|---|
| | BEF 2′ | BEF 3′ | BEF 2′ | BEF 3′ |
| 1st lead BEF | 1.22 | 0.128 | 0.918 | 0.552 |
| 2nd lead BEF | 0.0187 | 1.01 | −0.138 | 0.705 |
| WEF 1 | 0.157 | −0.0477 | −0.0251 | −0.181 |
| WEF 2 | 0.326 | −0.0393 | 0.464 | −0.458 |
| WEF 3 | 0.107 | −0.151 | 0.315 | 0.0681 |
| WEF 4 | 0.126 | −0.0468 | 0.216 | −0.0052 |

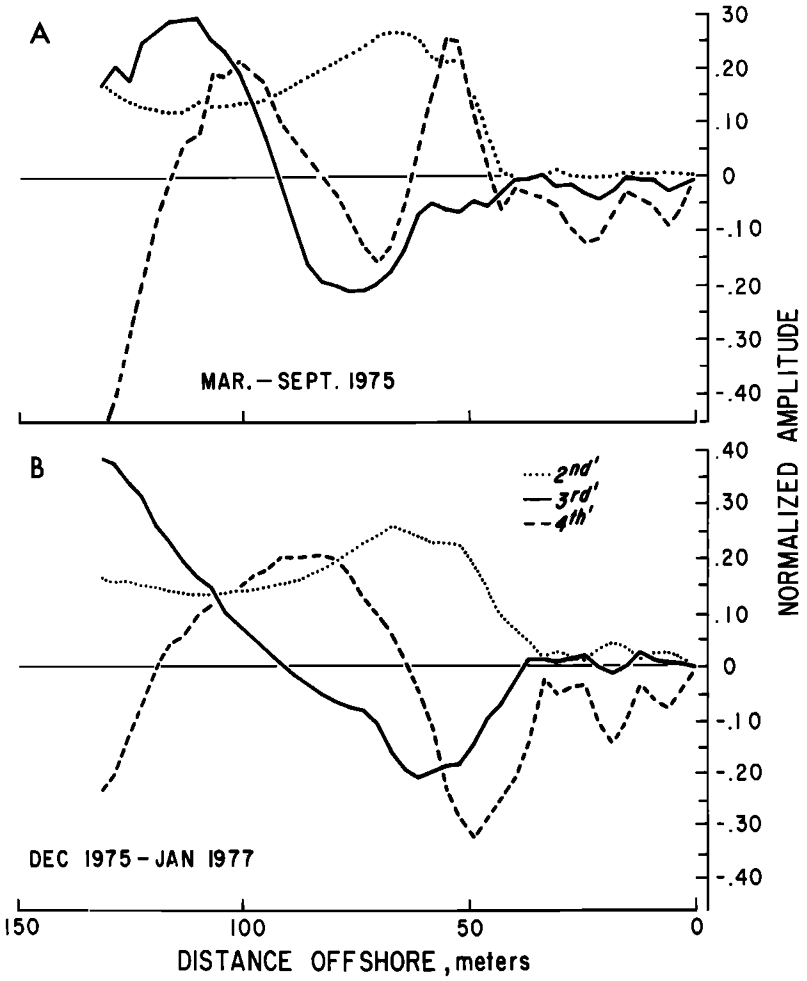


Fig. 10. The spatial structure of the beach eigenfunctions for North range for the periods of (*a*) March–September 1975 and (*b*) December 1975 through January 1977. The mean profiles have been removed from the data sets.

the prediction does not gradually deteriorate as the forecast progressed.

The results show that the best predictors represent a balance between adequate information about previous profile history and wave behavior and artificial predictability. The best forecaster appears to be the mean energy parameter, combined with the lead eigenfunction for the first BEF (2′). The higher-order BEF are not predictable and are better estimated by using the mean value of their time behavior, leading to a lesser mean square forecast error than the linear predictor estimate. Plots of the time dependence of the eigenfunctions $c_i(t)$ for different data sets compared with the prediction estimates display trends in the prediction (Figures 11 and 12). Extrema in the predictand are not well predicted, but trends are well predicted.

The total mean square value of the data for North range over the period March–September 1975 is 0.0114 m². The forecast in Figure 11 has a mean square forecast error of

TABLE 4. Percent of Variance Explained by the Second Through the Sixth Beach Eigenfunctions

| | North Range | | South Range | |
|---|---|---|---|---|
| | $n_t = 50$ | $n_t = 21$ | $n_t = 50$ | $n_t = 21$ |
| BEF | | | | |
| 2′ | 75.2 | (85.2) | 75.2 | (84.1) |
| 3′ | 13.0 | (6.4) | 10.4 | (7.0) |
| 4′ | 4.1 | (2.8) | 4.4 | (3.2) |
| 5′ | 2.9 | (1.9) | 4.0 | (2.3) |
| 6′ | 1.7 | (1.6) | 1.6 | (1.1) |
| Total | 96.9 | 97.9 | 95.6 | 97.7 |
| Variance without 1st BEF, m² | 0.0279 | 0.0134 | 0.0565 | 0.0827 |
| Percent of total mean square value of data accounted for by 1st BEF | 99.13% | 99.48% | 95.82% | 97.1% |

The numbers in parentheses are for the period March–September 1975. Other numbers are for the period December 1975 through January 1976; $n_x = 44$.

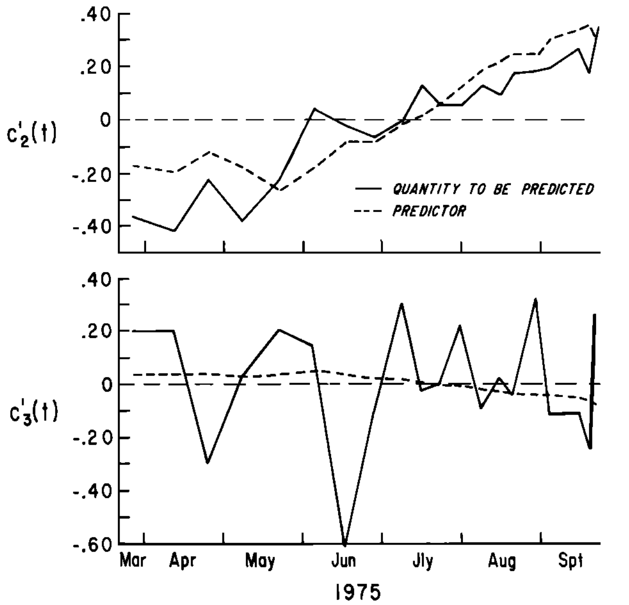


Fig. 11. A forecast of the temporal BEF for North range during the period of March–September 1975. The data consisted of one lead BEF and the square root of the mean energy value. The mean profile has been removed from the beach profile data set.

0.0037 $m^2$. The total mean square value of the input data for North range over the period of December 1975 through January 1977 is 0.021 $m^2$. The data in Figure 12 has a mean square forecast error of 0.0039 $m^2$.

Table 5 shows the trends in the prediction. The second lead BEF is positively weighted for predicting the second BEF, so there is a positive correlation between the previous profile and the current profile. The second lead BEF is negatively weighted for the third BEF, so there is a negative correlation between the second lead BEF and the current value of the third BEF. The square root of the mean weekly energy (the rms wave height) is negatively weighted with respect to the second

TABLE 5. Coefficient Matrices for Figures 11 and 12

| | Figure 11 | | Figure 12 | |
|---|---|---|---|---|
| | BEF 2′ | BEF 3′ | BEF 2′ | BEF 3′ |
| 1st lead BEF | 0.703 | −0.169 | 0.842 | −0.108 |
| $\bar{E}^{1/2}$ | −0.332 | 0.0014 | −0.238 | −0.435 |

BEF. This means that a large positive value of the wave height will correspond to a negative value of the second BEF or an erosional profile. Similarly, a negative (i.e., smaller than the mean) value of the wave height will yield a positive value of the second BEF, indicating that the beach is at an accreting stage.

As a more physical illustration, three measured profiles, spaced throughout the prediction period (Figure 12), are compared to estimates (Figure 13) derived from the linear predictor model (using (7) to recreate the profiles). Seasonal changes between measured profiles range up to 1 m or more for the profiles of February 27, 1976, and November 5, 1976. The predicted profile for all three cases is extremely close to the measured profile (always within 15 cm). Considering this a forecast and the measured profile was assumed to be unknown in the analysis, the predictor does a remarkable job at forecasting seasonal beach changes.

To show the importance of the forcing term in the prediction, hindcasts and forecasts were made by using only the lead BEF's as data, with no wave forcing. Although hindcast skill was comparable, forecast skill was considerably reduced, with the mean square forecast error more than doubled when the wave forcing was omitted. Similar results were obtained when random noise was added to the wave measurements. This numerical experiment reinforces the interpretation of the prediction results.

### *Application to Other Beaches*

These prediction techniques must be applied to other beaches to evaluate better the matrix of coefficients, **A**, as well

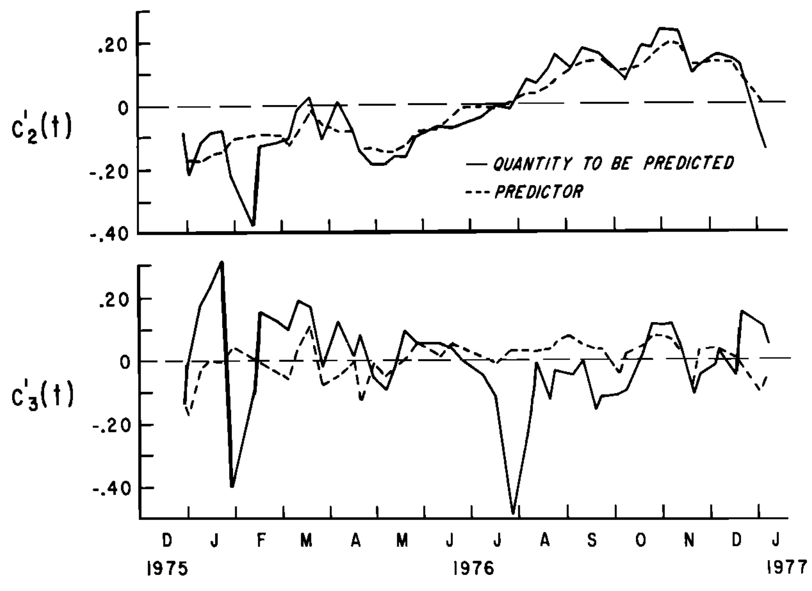


Fig. 12. A forecast of the temporal BEF for North range over the period of December 1975 through January 1977. The input data consisted of one lead BEF and the square root of the mean weekly energy value. The mean profile was removed from the beach profile data set.

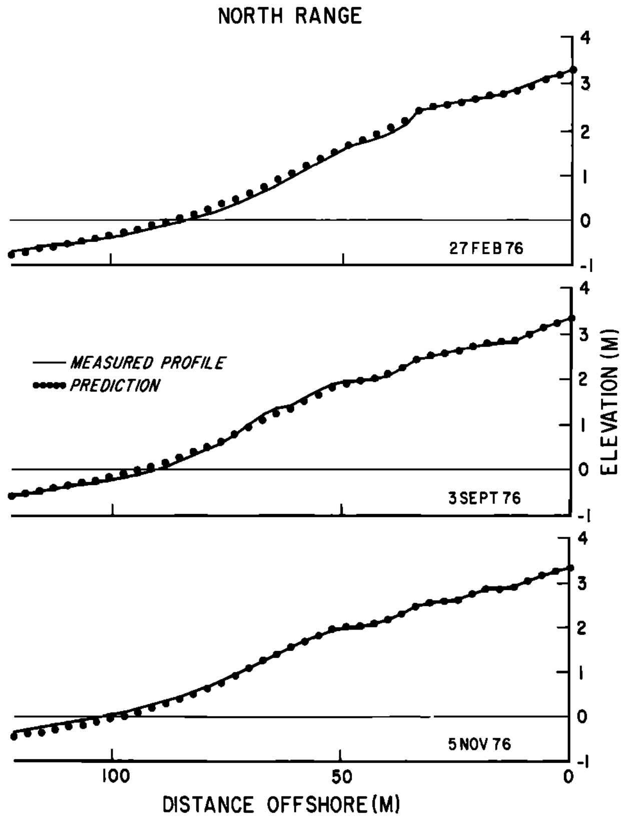


Fig. 13. A comparison of three measured beach profiles with the profile forecast using the linear predictor analysis.

as increase the statistical reliability of the estimators. The primary requirements for this type of statistical study are good wave estimates and profile data taken on at least a weekly basis to preserve predictability. Prediction of monthly beach changes is hampered by too great a smearing of wave information resulting from averaging wave characteristics over such a time scale. Beach sampling on a daily basis would be desirable and should be done eventually to improve this model, but it is seldom possible because of high costs and manpower requirements.

The wave data should consist of high-frequency samples of some characteristic wave parameters. At this time the statistical model is not sufficiently tuned to merit high-resolution directional spectral estimates, but frequency spectra can be applied to the model. Wave energy and frequency information must serve as inputs to the model, on both experimental and physical bases at least. The observations of these quantities should be made frequently enough to avoid aliasing. Visual wave observations can serve to form a crude estimate but are less desirable than spectral estimates.

Since it is known that other physical factors play a dominant role in beach response to incident waves, these factors can be examined once the statistical model is ready for fine scale interpretation. Other factors, such as grain size and beach slope, have to be examined for their role in the seasonal beach movement. One advantage of using the eigenfunction representation of beach data is that parameters such as grain size and beach slope are efficiently incorporated into the analysis; the spatial eigenfunctions directly reflect the influence of these parameters.

## CONCLUSIONS

Daily beach changes were predicted by spectral wave characteristics to a significant degree. Spectral representations of wave energy, radiation stress, energy flux, and wave steepness forecasted beach changes equally well. A longer data set is required to select one of the parameterizations over the others, because statistical reliability is low for the case studied. The lack of error propagation in the prediction is thought to reflect the inherent predictability of the beach change process. Only the second eigenfunction (BEF) representing seasonal beach changes is significantly predictable.

Weekly beach changes were predicted to a significant degree by weekly averaged wave characteristics. The mean energy between profile measurements and its square root were the best predictors of those tested; the other parameterizations worked well also. A large value of the energy predicts an erosional or bar profile; a low value predicts an accretionary or berm profile. A longer data set would increase the predictability and decrease the mean square forecast error. In addition, a longer data set would allow for a better determination of the 'optimal' beach forcing parameter.

The method of linear statistical estimation is applicable to predictions of beach profile changes for other beaches. Wave and weekly profile data from at least 1 year are required to determine the coefficient matrix to a high degree of accuracy. It is hoped that a data set consisting of daily profile measurements combined with spectral estimates of the wave field will be available in the future to test more rigorously this statistical technique.

The three dimensionality of the nearshore zone places an upper limit on the predictability of the beach profile changes. Comparison of profile changes at different ranges along a straight stretch of beach indicate that even here a longshore variation in beach response exists. This longshore variation may be due, in part, to minor convergences and divergences of the wave field alongshore. Despite the three-dimensional nature, beach profile changes were significantly predictable at Torrey Pines Beach, California. The influence of beach slope, grain size, etc. needs to be properly evaluated in the future.

*Acknowledgments.* This work was part of the first author's (D.G.A.) doctoral dissertation and was supported by the Office of Naval Research under contract with Scripps Institution of Oceanography, University of California, La Jolla, California. M. Clark helped design and draft the figures. A great number of people helped collect the mass of data required for this study; their help is gratefully acknowledged. W. D. Grant and W. K. Smith reviewed and considerably improved the manuscript. Contribution Number 4417 of the Woods Hole Oceanographic Institution, Woods Hole, Massachusetts.

## REFERENCES

Aubrey, D. G., Statistical and dynamical prediction of changes in natural sand beaches, Ph.D. dissertation, 194 pp., Scripps Inst. Oceanogr., San Diego, Calif., 1978.

Aubrey, D. G., Seasonal patterns of onshore/offshore sediment movement, *J. Geophys. Res., 84,* 6347–6354, 1979.

Aubrey, D. G., D. L. Inman, and C. E. Nordstrom, Beach profiles at Torrey Pines, California, *Proc. 15th Coastal Eng. Conf.,* 1297–1311, 1976.

Bowen, A. J., D. L. Inman, and V. P. Simmons, Wave 'set-down' and 'set-up,' *J. Geophys. Res., 73*(8), 2569–2577, 1968.

Davis, R. E., Predictability of sea surface temperature and sea level pressure anomalies over the North Pacific Ocean, *J. Phys. Oceanogr., 6*(3), 249–266, 1976.

Davis, R. E., Techniques for statistical analysis and prediction of geophysical fluid systems, *Geophys. Astrophys. Fluid Dyn.*, *8*, 245–277, 1977.

Inman, D. L. and G. A. Rusnak, Changes in sand level on the beach and shelf at La Jolla, California, *Tech Memo 82*, pp. 519–582 Beach Erosion Board. U.S. Army Corps of Eng., Washington, D. C., 1956.

Liebelt, P. B., *An Introduction to Optimal Estimation*, 273 pp., Addison-Wesley, Reading, Mass., 1967.

Longuet-Higgins, M. S., and R. W. Stewart, Radiation stress in water waves—A physical discussion with applications, *Deep Sea Res.*, *11*, 529–562, 1964.

Lorenz, E. N., Empirical orthogonal functions and statistical weather prediction, *Rep. 1*, 49 pp., Statistical Forecasting Project, Dept. of Meteorol., Mass. Inst. of Tech., Boston, 1959.

Lowe, R. L., D. L. Inman, and B. M. Brush, Simultaneous data system for instrumenting the shelf, *Proc. 13th Conf. Coastal Eng.*, 95–112, 1973.

Nordstrom, C. E., and D. L. Inman, Sand level changes on Torrey Pines Beach, California, *Eng. Misc. Pap. 11-75*, 166 pp., Beach Erosion Board U. S. Army Corps of Eng., Fort Belvoir, Va., 1975.

Pawka, S. S., D. L. Inman, R. L. Lowe, and L. C. Holmes, Wave climate at Torrey Pines Beach, California, *Tech Pap. 76-5*, 372 pp. Beach Erosion Board U. S. Army Corps of Eng., Fort Belvoir, Va., 1975.

Resio, D., B. Hayden, R. Dolan, and L. Vincent, Systematic variations in offshore bathymetry, *Tech. Rep. 9*, 28 pp., Univ. of Va., Charlottesville, 1974.

Seymour, R. J., and M. H. Sessions, Regional network for coastal engineering data, *Proc. 15th Coastal Eng. Conf.*, 60–71, 1976.

Vincent, C. L., and D. T. Resio, An eigenfunction parameterization of a time sequence of wave spectra, *Coastal Eng.*, *1*, 185–205, 1977.

Winant, C. D., D. L. Inman, and C. E. Nordstrom, Description of seasonal beach changes using empirical eigenfunctions, *J. Geophys. Res.*, *80*(15), 1979–1986, 1975.

(Received August 10, 1979;
revised December 14, 1979;
accepted December 17, 1979.)